Journal of New Technology and Materials (JNTM)
J. New Technol. Mater.
Vol. 10, N°01 (2020)50-55

OEB Univ. Publish. Co.

Hydrogen diffusion mechanism in polysilicon solar cells deduced from analysis of dopant deactivation and open-circuit voltage evolution

Djamel Madi[a*], and Djameleddine Belfennache[b]

[a]*Laboratory of Materials and Sustainable Development, Faculty of Sciences and Applied Sciences, Mohand Oulhadj University, Bouira, 10000, Algeria*
[b]Research Center in Industrial Technologies (CRTI), P.O. Box 64, Cheraga 16014 Algiers, Algeria

*Corresponding author, email: madidjamel@yahoo.com

Received date: Nov. 09, 2019; accepted date: May 07, 2020

Abstract

The present work reveals a hydrogen diffusion mechanism in a polysilicon solar cell in order to achieve an effective passivation of defects and then high photovoltaic conversion efficiency. Plasma hydrogenation treatments were performed on polysilicon and monosilicon solar cells to witness, respectively, the evolution of the open-circuit voltage and the boron activation profile. The results obtained show clearly that the open-circuit voltage improves as the microwave plasma power increases. Nevertheless, the measured values are much higher for a less doped phosphorus emitter, which confirms that the hydrogen diffusion in the bulk of silicon is more prevented as well as the level of doping is high. However, the tendency of the open circuit-voltage values to saturation at high microwave plasma powers indicates that hydrogen can also produce new defects in polysilicon. This last observation has been well verified on monosilicon n$^+$p solar cells. Also, hydrogen neutralizes boron and generates a concentration gradient between the boundary of the space charge zone and the depth of the p base region. As a result, we have admitted the existence of an electric field that encourages deep hydrogen diffusion atoms in the bulk of polysilicon. Moreover, the appropriate analysis of these results allowed us to propose a credible mechanism for hydrogen diffusion in polysilicon solar cells.

Keywords: solar cell; boron deactivation; hydrogenation; open-circuit voltage; hydrogen diffusion.

1. Introduction

The rapid growth of global energy demand encourages the development of photovoltaic energy. However, it faces two challenges: low cost and high conversion efficiency. These last two qualities can be achieved by referring to polysilicon-based solar cells (poly-Si) provided that the activity of impurities and inter and intra-grain defects is effectively passivated with hydrogen. Several papers have published results of the hydrogenation of poly-Si [1-3] based n$^+$pp$^+$ solar cells where a particular attention has been dedicate to the methods used to introduce hydrogen into cells across the emitter region n$^+$ and experimental conditions leading to high values of open-circuit voltage (V_{oc}). Nevertheless, the hydrogenation treatments modify the level of doping of the base region p resulting from the formation of the dopant-hydrogen complexes [4-12]. Despite the active concentration of the dopant being a crucial parameter that defines the electrical properties of a solar cell, no study has been done to relate the evolution of V_{oc} with the deactivation of the dopant to describe the hydrogen diffusion mechanism in n$^+$pp$^+$ poly-Si solar cell.

The exposure of the n$^+$ emitter region to the hydrogen flow is a current technique for the passivation of the different impurities and defects existing within the n$^+$ pp$^+$ cell. However, the amount of hydrogen introduced into the p region is greatly reduced by the presence of the phosphorus-doped n$^+$ layer due to platelet formation near the surface [13-15]. In addition, the deactivation of the doping atoms was well established from measurements of the capacitance-voltage characteristic (C-V) carried out on n$^+$p junctions following the variation of the doping profiles before and after hydrogenation [16-24]. However, during the formation of the n$^+$ emitter region, the phosphorus atoms tend to diffuse preferentially at the grain boundaries [25, 26], which would lead to the formation of non-flat junctions within the polycrystalline silicon films, so it is impossible to determine the active phosphorus concentration from the C - V measurements. Also, since the deactivation of dopant atoms and the passivation of defects coexist simultaneously in hydrogenated poly-Si films; our approach is to study them independently. As a result, monocrystalline silicon films (free of defects) doped uniformly with boron are used for the elaboration of the n$^+$p junctions in order to analyze the mechanism of deactivation of the dopant by hydrogen and on the other hand, the monitoring evolution of the open-circuit voltage (V_{oc}), measured on n$^+$pp$^+$ solar cells in hydrogenated poly-Si, is dedicated to the examination of the passivation of inter and intra-grain defects.

2. Experimental

Figure 1 shows the PECVD Roth & Rau reactor (Plasma Enhanced Chemical Vapor Deposition) used for the hydrogenation treatments available at the ICUBE laboratory (previously named INESS) in Strasbourg (France). It consists of a chamber with two aligned compartments and in contact; the walls are cooled by a water flow. The first compartment is located in the upper part of the chamber below a quartz window separating it from the waveguide carrying a microwave excitation frequency of 2.45 GHz with variable powers ranging from 100 to 650W. In addition, it is surrounded by magnetic bobbins traversed by an electric current of 5A for the creation of a magnetic field of 0.0875 Tesla in an area called "resonance zone". This field is used for the implementation of a microwave plasma discharge assisted by electron cyclotron resonance (MW-ECR). An arrival of the plasma gases (Ar, H_2, NH_3 and N_2) is placed upstream of the plasma excitation zone.

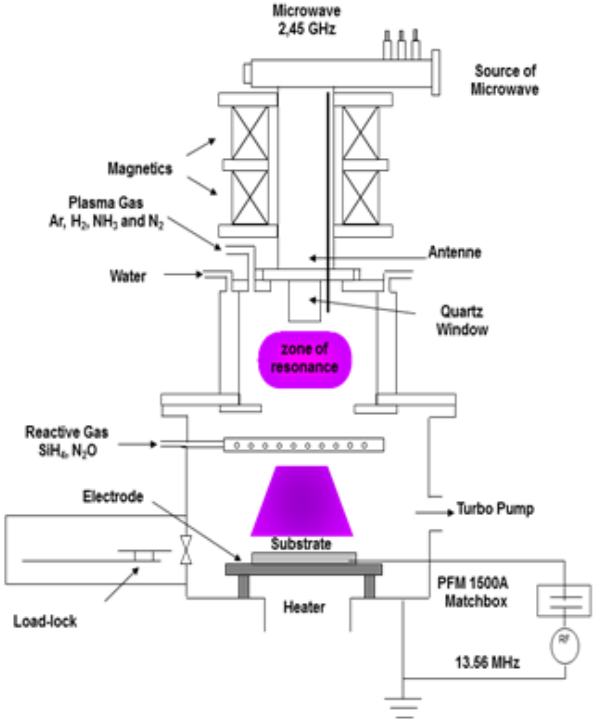

Figure 1. Vertical schematic of the PECVD Roth and Rau reactor used for hydrogenation treatment [11].

However, the second compartment is located in the lower part of the chamber (called the deposition chamber) and it is used for radiofrequency discharges and confinement of free species of plasma gases. It contains a circular electrode (radiofrequency antenna) and a graphite substrate 150mm in diameter, connected to ground and heated by an electrical resistor. The substrate temperature is measured with a pyrometer placed directly under the sample and in the middle of the graphite substrate. A sluice valve separates this compartment from the load lock chamber, which serves for loading and unloading samples without losing the high vacuum of the reactor chamber. The vacuum in the load lock is realized by a mechanical pump. Finally, the by-products of the chemical reactions are evacuated thanks to a turbo-molecular pump, purged by a flow of nitrogen in order to protect its most sensitive parts.

The polysilicon films were prepared on thermal SiO_2 substrates by the Rapid Thermal Chemical Vapor Deposition (RTCVD) technique at atmospheric pressure and a temperature of 1080°C, using trichlorosilane and diborane as precursor and doping gas, respectively. This results in the superposition of two boron doped layers: p (base region) and p^+ (back surface field region) having thicknesses, respectively, of 3.5 µm doped at 3×10^{16} cm^{-3} and 0.5µm doped at 5×10^{19} cm^{-3}. Optical microscopy revealed, after polishing and Secco etching for 15 sec, the image of figure 2 where we can see a polycrystalline structure with grain sizes of about 0.3 to 2.3 µm distributed in a less uniform manner on all the surface of the films.

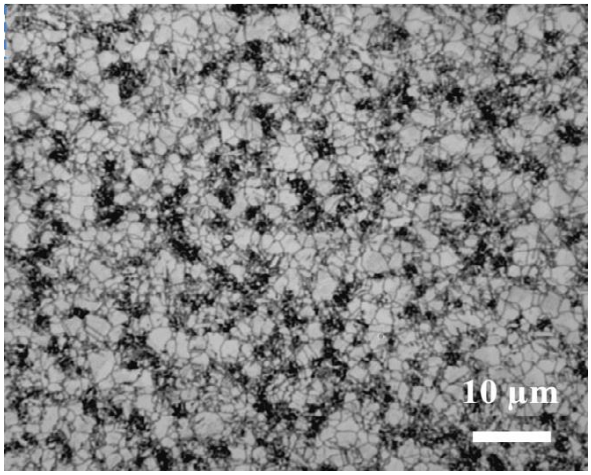

Figure 2. Surface image of a polysilicon layer deposited by RTCVD.

The emitter n^+ region was formed by thermal diffusion of phosphorus at 900°C for 60 min from a doping source P507 or P509. This results in a distribution of P atoms according to the complementary error function (erfc) with a surface concentration ranging from $5x10^{20}$ to $2\times10^{21}cm^{-3}$ and a junction depth of about 0.5 to 0.8µm. After the diffusion process, the samples are soaked in an HF hydrofluoric acid bath (5%) for two minutes to remove oxide residues of the doping source. Then, they are rinsed with deionized water and dried under nitrogen flux. An average sheet resistance of 30 Ω/sq was measured by the four-point probe technique on the n^+ emitter region.

Furthermore, the measurements of the open circuit voltage (V_{oc}) on our n^+pp^+ solar cells require the realization of the contacts with the emitter (n^+) and the back surface field (p^+). However, the presence of the SiO_2 insulating layer in the structure requires that all contacts be taken on the front side only, which leads to the formation of a mesa diode by the SCMP (side-contacted mesa process) process. Access to the p^+ region was achieved by reactive ion etching (RIE), where SF_6 gas etches the n^+p layer at a rate of 1.6 µm/min, forming a mesa cell.

Also n^+p junctions were made on FZ <100> monocrystalline silicon and doped with boron at 3.10^{15} cm^{-3}. A thin n^+ region about 0.15µm thick was made by diffusion of phosphorus from P507 at 900°C for 15min. After chemical cleaning of the n^+p diodes, these latter were transferred to the MW-ECR reactor to endure a hydrogenation treatment through the exposure of the n^+ surface to the hydrogen plasma. Discharged from the PECVD reactor, they are cleaned in a bath of hydrofluoric acid HF (2%) for 2 min followed by rinsing with deionized water and finally dried under nitrogen flux. On the hydrogenated faces, we deposited a mask having square openings of $1mm^2$ and separated from each other by a distance of 1mm. This step was followed by the introduction of the samples in a thermal evaporator to deposit $1mm^2$ square section of aluminum (Al) layer with 0.1µm thick through the mask openings. An etching step of n^+ layer uncovered by Al was carried out using a "RIE" reactor in which a cold plasma is produced by a radio frequency capacitive discharge (f = 13.56MHz , P_{rf} = 150W) in SF_6 gas under a low pressure of 6.6×10^{-3} mbar. Then, we carried out a vacuum evaporation of 0.1µm thick gold (Au) layer on the entire back surface. The CV measurements performed on n^+p junctions were obtained from an HP4192A impedance analyzer available in the ICUBE laboratory. After duration of 15min, necessary for the stabilization of the C-V equipment, the inverse polarization of the n^+p diodes operates at ambient temperature under inverse voltages ranging from 0 to 5V with a step of 0,1V and a frequency of 1MHz. The program dedicated for capacity measurement versus applied voltage records the results as data files and then treated in the Origin 6.0 graphics software to extract the doping profile through the equations reported in reference [27].

3. Results

Grain boundary activity can be demonstrated by measuring the open-circuit voltage (V_{oc}) on n^+pp^+ polysilicon (poly-Si) solar cells and comparing it with that obtained from n^+p monosilicon structures (mono-Si). The results obtained are shown in Table 1. It is clearly seen that the V_{oc} values measured on mono-Si cells are much higher compared to those obtained on poly-Si cells. These are mainly due to the effect of grain boundary defects that degrade the electrical properties of the polysilicon layers. Indeed, due to interface states localized in space of the bandgap, the grain boundaries have doubly detrimental effects on the performance of electronic devices as compared to the characteristics of single crystal silicon devices. On one side, the trapping states of majority carriers give rise to an energy barrier which hinders the movement of free carriers from one grain to another, which limits the conductivity in the polycrystalline silicon and on the other hand, the preferential diffusion of phosphorus at grain boundaries gives rise to a wide space charge region, which further increases the saturation current in this area [28]. Another mechanism that most certainly contributes to the recombination current of minority carriers, thus limiting their lifetime, comes from places where a vertical grain boundary crossing the space charge zone of the junction [29]. Even if these crystalline defects are at the origin of a higher absorption of the light compared to the grain, this very slight benefit can be neglected in the poly-Si characterized by a grain size of the order of 1 µm, in consideration of the degradation of the transport properties they cause.

Table1: Open-circuit voltage measured on monosilicon and polysilicon based solar cells for two types of doping sources P507 and P509. Thermal diffusion of phosphorus to form the emitter region n^+ was at 900°C and 60 min.

	Open-circuit voltage : V_{oc} (mV)	
Doping sources	P507	P509
Mono-Si : n^+p	550 ± 10	555 ± 10
Poly-Si : n^+pp^+	213 ± 5	155 ± 5

In addition, while the open-circuit voltage measured on n^+p mono-Si structures is not influenced by the conditions of the emitter formation, the situation is completely different in the case of n^+pp^+ poly-Si solar cells. This observation is explained by the fact that during emitter formation on polycrystalline films, two phenomena are responsible for improving the electrical properties of the material. This is the passivation by phosphorus of grain boundary defects and removal of impurities by Getter effect from the poly-Si bulk to inactive areas of the device [30-32].

3.1. MW-ECR plasma hydrogenation effect on deactivation profile and open-circuit voltage evolution

The hydrogenation treatments of the n^+pp^+ poly-Si solar cells were carried out in the PECVD reactor by exposing the region of the n^+ emitter to the MW-ECR hydrogen

flux. Figure 3 shows the open-circuit voltage (V_{oc}) measured as a function of the microwave plasma power (P_{MW}). After 1 hour of hydrogenation at 400°C, a significant and continuous increase of V_{oc} is observed for the two doping sources P507 and P509 of the n^+ emitter region. This enhancement of V_{oc} is due to hydrogen passivation of grain boundary defects and suppression of band tails that act as barriers for majority carriers and recombination sites for minority carriers. However, the recorded V_{oc} values are higher for P507 than for P509. In addition, the effect of the emitter doping level on V_{oc} values is more evident at low P_{MW}, whereas at high values they are approximately similar for both doping sources. Indeed, V_{oc} is close to 340mV at P_{MW}=650W. This result is in good agreement with those reported elsewhere [32] where it has been observed that hydrogen diffusion in the bulk of silicon is well prevented as the phosphorus concentration is high in the material. However, the tendency of the V_{oc} values to saturation for the two doping levels P507 and P509 as P_{MW} is high is probably due either to the formation of H_2 molecules that manifest as platelets near the surface of n^+ having the effect of suppressing the hydrogen diffusion in the polysilicon bulk or to the generation of defects within grains that degrade the electrical properties of the photovoltaic device.

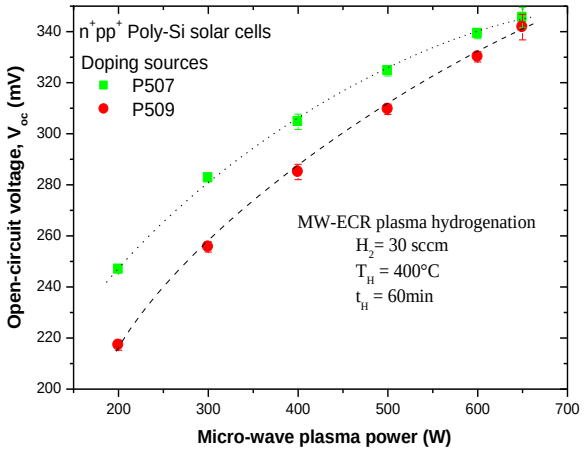

Figure 3. Effect of the power of the MW-ECR hydrogen plasma on the open circuit voltage measured on n^+pp^+ poly-Si solar cells. The n^+ emitter formation was by thermal diffusion from the doping sources P507 and P509.

To clarify which of these processes is responsible for V_{oc} saturation, we performed MW-ECR plasma hydrogenation on n^+p monocrystalline silicon solar cells. We noted a decrease in V_{oc} especially significant that P_{MW} is high (see Figure 4). The behavior of V_{oc} gives evidence that passive hydrogen defects but in counterpart it can create new defects. Indeed, many researchers reported that when the hydrogenation is excessive, the hydrogen concentration could exceed that of dangling bonds by about two orders of magnitude [34-35]. The excess hydrogen can react with the low energy Si-Si bonds to lead to the formation of Si-H complexes. However, a hydrogen atom involved in a Si-Si bond produced a Si-H compound and a dangling bond Si-. Other possible defects induced by excessive hydrogenation are the defects involving the formation of molecular hydrogen within the silicon grains according to the following configuration advanced in the literature [36-38]: Si-H + H = Si- + H_2 or Si-H + H + = Si + + H_2. Thus, optimization of the hydrogenation process is important.

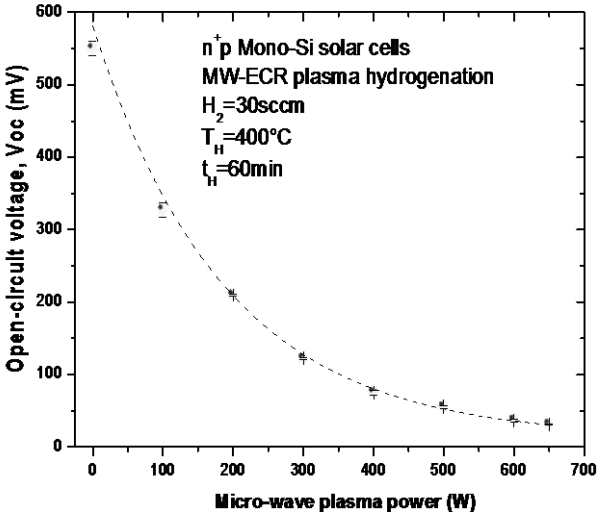

Figure 4. Effect of the power of the MW-ECR hydrogen plasma on the open-circuit voltage of n^+p mono-Si solar cells. n^+ emitter formation was by thermal diffusion from the P509 solution for 60 min.

Also, the doping profiles resulting from the C-V measurements of the mono-Si n^+p junctions show that the MW-ECR hydrogen plasma induces a deactivation of the boron in the silicon. In fact, figure 5 reveals a deactivation rates that are even higher as the microwave plasma power is important compared with a uniform boron distribution in bulk of the non-hydrogenated n^+p junctions. In addition, the active boron profiles after hydrogenation show concentration gradients between the space charge zone (ZCE) boundary and the depth of the p region. Consequently, we can admit the existence of a deep diffusion of hydrogen atoms in the bulk of the p region due to the electric field caused by the concentration gradient.

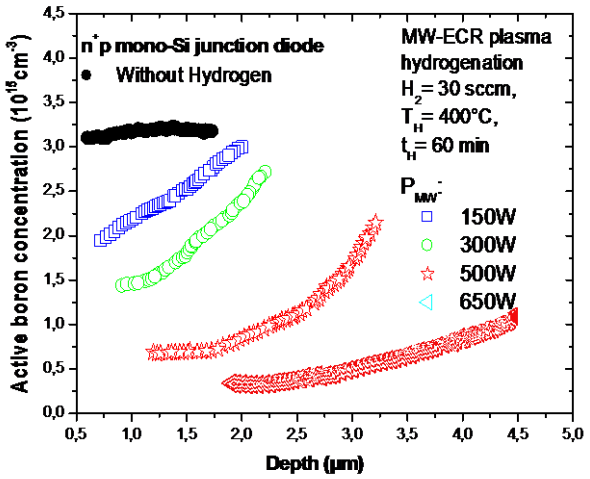

Figure 5. Active boron concentration profiles as a function of depletion depth at various microwave plasma power.

In addition, boron deactivation occurs in an electrically neutral region that acts as a low mobility resistive buffer layer near the junction, resulting in a reduction in the number of charge carriers that recombine at the interface and at the edge of the photovoltaic cell, which is in good agreement with our results where V_{oc} improves as the concentration of inactive boron is high.

3.2. Hydrogen diffusion mechanism in n^+pp^+ poly-Si solar cell

Although a MW-ECR hydrogen plasma is characterized by a high density of H^- atoms that reach the n^+ surface of the solar cell as the microwave discharge power increases [4], the question to ask is what mechanism hydrogen diffuses from the n^+ surface to the bulk of the base p region? According to Johnson [39], the state of hydrogen charge (H^+, H^- and H^0) in the silicon depends on the position of the Fermi level in the band gap. It has been speculated that the conversion $H^+ \leftrightarrow H^-$ occurs via H^0 [39, 40]. Moreover, H^0 species have a very high diffusion coefficient with respect to the capture of an electron or other H^0 to give, respectively, H or H_2. Therefore, H^- absorbs an electron e^- at the surface of n^+ and becomes H^0 and subsequently it diffuses towards the p region without any Coulomb barrier to overcome [39]. After crossing the ZCE, a neutral hydrogen atom would be ionized by capture of a free hole ($H^0 + h^+ \rightarrow H^+$) and continue to diffuse as a proton in the p-type substrate. Then, the deactivation of boron would progress with $H^+ + B^- \rightarrow BH$, which is consistent with the overall chemical reaction given elsewhere [39-44]. On the other hand, the reactions $H^0 + h^+ \rightarrow H^+$ and $H^+ + B^- \rightarrow BH$ can take place from the edge of the ZCE. Therefore, the boron deactivation rate is highest near the ZCE compared to the depth of the p region. Thus, the presence of the acceptor concentration gradient would result in an electric field, which promotes the diffusion of H^+ in the depth of p base. Gradually, as the microwave power increases, the H^- migration in the bulk of the p region becomes higher due to the enhance in the concentration gradient. Although the mechanism of hydrogen diffusion in polysilicon is different from that of monosilicon [45], our results suggest that the passivation of defects in polysilicon is governed by the ability of hydrogen to diffuse into the material instead of forming H_2 type defects.

4. Conclusion

In this work, we tried to propose a mechanism for hydrogen diffusion in n^+pp^+ polysilicon solar cell for effective defects passivation and then achieve high photovoltaic conversion efficiencies. To do this, we carried out MW-ECR hydrogenation treatments on n^+pp^+ poly-Si solar cells and on n^+p mono-silicon diodes in order to follow, respectively, the open-circuit voltage (V_{oc}) evolution and the boron deactivation profile in the p base region. Our results clearly show that V_{oc} values increase significantly as the microwave discharge power (P_{MW}) is high. However, the measured values are higher on cells having n^+ emitters formed with the P507 solution compared to those of P509. This result confirms that hydrogen diffusion in the bulk of silicon is thereby prevented that phosphorus concentration is high in the crystalline material. However, the trend of V_{oc} values saturation at high microwave discharge powers demonstrates that hydrogen can also generate new defects in the polysilicon. This last observation has been well confirmed on n^+p monosilicon solar cells. Also, the hydrogen neutralizes the boron and generates a concentration gradient between the limit of the space charge zone and the depth of the p region. Consequently, we have admitted the existence of an electric field which activates a deep diffusion of hydrogen H^- atoms in the p region bulk. Thus, during the hydrogenation of the n^+p cells, the H^- ions arrive at the n^+ surface where they absorb an electron and become H^0 atoms and subsequently it diffuses towards the p region without any Coulomb barrier to overcome. After crossing the ZCE, a neutral hydrogen atom would be ionized as an H^+ by the capture of a free hole h^+. Subsequently, boron deactivation progressed from the edge of the ZCE. As a result, the higher boron deactivation rate near the ZCE compared to the depth of the p region gives rise to an acceptor concentration gradient that results in the existence of an electric field that promotes H^+ diffusion in the bulk of p base and later the passivation of the defects.

Acknowledgments

The author would like to express their thanks to the personnel of the ICUBE (Formerly InESS) Laboratory of Strasbourg-France for their help and cooperation.

References

[1] L. A. Verhoef, P. Michiels, W. C. Sinke, C. M. M. Denisse, M. Hendriks, R. J. C. Van Zolingen, Appl. Phys. Lett. 57 (1990) 2704.
[2] K. Nishioka, T. Yagi, Y. Uraoka, T. Fuyuki, Sol. Energy Mater. Sol. Cells 91 (2006) 1.
[3] L. Carnel, I. Gordon, K. Van Nieuwenhuysen, D. Van Gestel, G. Beaucarne, J. Poortmans, Thin Solid Films 487 (2005) 147.
[4] D. Madi, P. Prathap, A. Slaoui, Appl. Phys. A 118 (2015) 231.
[5] D. D. Madi, A. Focsa, S. Roques, S. Schmitt, A. Slaoui, B. Birouk, Energy Procedia 2 (2010) 151.
[6] N. H. Nickel, N.M. Johnson, W.B. Jackson, Appl. Phys. Lett. 62 (1993) 3285.
[7] S. J. Pearton, J.W. Corbett, T.S. Shi, Appl. Phys A 43 (1987) 153.
[8] T. Zundel, A. Mesli, J.C. Muller, P. Siffert, Appl. Phys. A 48 (1988) 31.
[9] T. Zundel, J. Weber, Phys. Rev. B 39 (1989) 13549.
[10] T. Zundel, J. Weber, Phys. Rev. B 43 (1991)4361.
[11] A. Slaoui, E. Pihan, I. Ka, N.A. Mbow, S. Roques, J.M. Koebel, Sol. Energy Mater. Sol. Cells 90 (2006) 2087.
[12] D. Madi, P. Prathap, A. Focsa, A. Slaoui, B. Birouk, Appl. Phys. A 99 (2010) 729.
[13] N. M. Johnson, Phys. Rev. B 31 (1985) 5525.
[14] N. M. Johnson, M.D. Moyer, Appl. Phys. Lett. 46 (1985) 787.
[15] N. M. Johnson, F. A. Ponce, R. A. Street, R. J. Nemanich, Phys. Rev. B 35 (1987) 4166.
[16] S. K. Estreicher, L. Throckmorton, D. S. Marynick, Phys. Rev. B 39 (1989) 13241.
[17] N. M. Johnson, C. Herring, D.J. Chadi, Phys. Rev. Lett. 56 (1986) 769.
[18] K. Bergman, M. Stavola, S.J. Pearton, J. Lopata, Phys. Rev. B 37 (1988) 2770.
[19] N. H. Nickel, Microelectron. Reliab. 47 (2007) 899.
[20] N. Fukata, S. Sato, H. Morihiro, K. Murakami, K. Ishioka, M. Kitajima, J. Appl. Phys. 101 (2007) 461071.
[21] Y. Ma, Y.L. Huang, W. Düngen, R. Job, W.R. Fahrner, Phys. Rev. B 72 (2005) 085321.
[22] A. Royal, F. Mazen, F. Gonzatti, M. Veillerot, A. Claverie, Mater. Sci. Semicond. Process 67 (2017) 118.
[23] R. E. Pritchard, M.J. Ashwin, J.H. Tucker, R.C. Newman, E.C. Lightowlers, M.J. Binns, S.A. McQuaid, R. Falster, Phys. Rev. B 56 (1997) 3161.
[24] K. Murakami, N. Fukata, S. Sasaki, K. Ishioka, M. Kitajima, S. Fujimura, J. Kikuchi, H. Haneda, Phys. Rev. Lett. 77 (1996) 3161.
[25] M. M. Mandurah, K. C. Saraswat and T. I. Kamins, IEEE Transactions on Electron Devices 28 (1981) 1163.
[26] A. D. Buonanquisti, W. Carter, P. H. Holloway, Thin Solid Films 100 (1983) 235.
[27] R. Rizk, P. de Mierry,D. Ballutaud, M. Aucouturier, D.Mathiot, Phys. Rev. B 44 (1991) 6141.
[28] G. Beaucarne, J. Poortmans, M. Caymax, J. Nijs, R. Mertens, IEEE Transactions on Electronics Devices 47 (2000) 1118.
[29] L. Carnel, I. Gordon, D. Van Gestel, D. Vanhaeren, P. Eyben, G. Beaucarne, J. Poortmans, IEEE Electron Device Letters 28 (2007) 899.
[30] J. Cheng, C. M. Shyu, K. M. Stika, Mat. Res. Soc. Symp. Proc.14 (1983) 383.
[31] A. Neugroschel, J. A. Mazer, IEEE Transactions on Electron Devices 29 (1982) 225.
[32] T. H. Di Stefano, J. J. Cuomo, Appl. Phys. Lett.30(1977) 351.
[33] D. Belfennache, D. Madi, N. Brihi, M. S. Aida, M. A. Saeed, Appl. Phys. A 124 (2018) 697.
[34] N. H. Nickel, N.M. Johnson, W.B. Jackson, Appl. Phys. Lett. 62(1993) 3285.
[35] T. Yamazaki, Y. Uraoka, T. Fuyuki, Thin Solid Films 487(2005) 26.
[36] D. L. Griscom, J. Appl. Phys. 58 (1985) 2524.
[37] D. M. Fleetwood, Microelectronics Reliability 42 (2002) 523.
[38] K. Kitahara, S. Murakami, A. Hara, K. Nakajima, Appl. Phys. Lett. 72 (1998) 2436.
[39] N. M. Johnson, Appl. Phys. Lett. 47(1985) 874.
[40] C. Herring, N. M. Johnson and C. G. Van de Walle, Phys. Rev. B 12 (2001) 125209-1.
[41] T. P. Sokrates, Appl. Phys. Lett. 50 (1987) 995.
[42] J. I. Pankove, P.J. Zanzucchi, C.W. Magee, G. Lucovsky, Appl. Phys. Lett. 46 (1984) 421.
[43] N. Fukata, S. Fukuda, S. Sato, K. Ishioka, M. Kitajima, T. Hishita, K. Murakami, Phys. Rev. B 72 (2005) 245209-1.
[44] P. J. H. Denteneer, C.G. Van de Walle, S.T. Pantelides, Phys. Rev. B 39 (1989) 10809.
[45] W. B. Jackson, N.M. Johnson, C.C. Tsai, I.W. Wu, A. Chiang, D. Smith, Appl. Phys. Lett. 61 (1992)1670.